Self-Aligning and Flexible Dielectric Waveguide Plug for MMICs at *G*-Band

Martin Geiger, *Student Member, IEEE*, Martin Hitzler, *Member, IEEE*, Winfried Mayer, *Senior Member, IEEE*, and Christian Waldschmidt, *Senior Member, IEEE*

***Abstract*— The packaging technology for transitions to dielectric waveguides in the frequency range above 100 GHz is complex and must be highly precise, and the waveguides are usually permanently connected. This letter presents a transition from a monolithic microwave integrated circuit (MMIC) to a flexible dielectric waveguide at *G*-Band (140–220 GHz), which is self-aligning and, thus, reduces the requirements for packaging accuracy. Furthermore, the transition is mechanically decoupled to avoid mechanical stress to the MMIC and to reconnect it arbitrarily often. A patch radiator on a quartz-glass carrier is excited by a coupler on the MMIC. It feeds the HE_{11} mode into a rigid, high-permittivity dielectric dome, which increases the coupling efficiency. The flexible dielectric waveguide is placed above the dome and fixed with Rohacell half shells. The minimum insertion loss measured with a back-end-of-line (BEOL) MMIC is 3.0 dB at 168 GHz.**

***Index Terms*— Dielectric waveguide, mechanical decoupling, monolithic microwave integrated circuit (MMIC), MMIC-to-dielectric waveguide transition, self-alignment.**

I. Introduction

Large bandwidths and low-cost SiGe monolithic microwave integrated circuits (MMIC) make the frequency range above 100 GHz attractive for both communication and radar. With flexible, low-loss dielectric-waveguide interconnects, mm-wave signals can be transmitted over long distances for board-to-board links [1] or to feed remote antennas [2], [3]. This opens up new fields of applications.

For this reason, several transitions from an MMIC to a dielectric waveguide have already been proposed in the literature for communication links [4]–[10]. Some transitions are based on the resonant structures like dielectric resonators [4] or patches [5] to feed the dielectric waveguide. Another transition excites a wave in the dielectric waveguide with a half-mode substrate integrated waveguide [6]. In order to couple the signal more efficiently into the dielectric waveguide, the used materials have a high permittivity, such as high-resistivity silicon ($\varepsilon_r = 11.9$). Furthermore, the materials are low-loss, rigid, and in permanent contact with the MMIC, as required for short-range chip-to-chip interconnects.

For applications with a signal transmission over several meters, the requirements for the transition and the dielectric waveguide are different. Due to the nonstatic scenario, a flexible waveguide made of Teflon or high-density polyethylene (HDPE) with a relative permittivity around 2.2 is necessary. Furthermore, a mechanical decoupling of the MMIC and the waveguide increases the transition robustness and allows reconnecting the MMIC and the waveguide several times. This can be realized by radiating into the dielectric waveguide [11], [12], with metallic waveguide adapters [13], or additional transitions to the printed circuit board (PCB) [14]. However, all approaches increase the insertion loss (IL) from the MMIC to the dielectric waveguide compared with the previously mentioned transitions.

This letter presents a mechanically decoupled transition from an MMIC to a flexible dielectric waveguide using a high-permittivity dielectric waveguide adapter to increase the coupling efficiency. Furthermore, the flexibility of the HDPE waveguide is used to align itself. The transition was designed and measured for a SiGe back-end-of-line (BEOL) MMIC. In the following section, the transition principle is explained. In Section III, the measurement results are shown and compared with the state-of-the-art designs.

II. Transition Principle

The transition from the SiO_2 back end ($\varepsilon_r = 4$, $\tan\delta = 0.02$, $h_{BEOL} = 10$ μm) to the flexible dielectric waveguide is composed of several components, as shown in Fig. 1(a).

In order to decouple the field efficiently of the back end, a $\lambda/2$-patch on a 100-μm-thick quartz-glass carrier ($\varepsilon_r = 3.8$, $\tan\delta = 0.001$) is placed above a shortened $\lambda/4$-patch, which is fed by a microstrip line on the back end [15] [see Fig. 2(b)]. The length l_{patch} of the $\lambda/2$-patch determines the center frequency f_0 of the transition. With a back-end area of only 170 μm × 220 μm = 0.01 λ_0^2, the transition has a very compact design, with λ_0 corresponding to the wavelength at f_0.

On the top of the patch, a round dielectric waveguide dome with the diameter $d_{PEEK} = 780$ μm is placed, in which the HE_{11} mode is excited. By increasing the permittivity of the dielectric waveguide, the field is decoupled more efficiently of the back end. The dielectric waveguide is made of polyetheretherketone (PEEK), since it is very simple to machine. Furthermore, the permittivity of $\varepsilon_r = 3.2$ ($\tan\delta = 0.006$) is high

Manuscript received December 16, 2019; accepted January 15, 2020. Date of publication February 17, 2020; date of current version March 11, 2020. This work was supported by the Ministry for Science, Research and Arts Baden-Württemberg, Germany, within the project ZAFH MikroSens. *(Corresponding author: Martin Geiger.)*

Martin Geiger and Christian Waldschmidt are with the Institute of Microwave Engineering, Ulm University, 89081 Ulm, Germany (e-mail: martin-2.geiger@uni-ulm.de).

Martin Hitzler and Winfried Mayer are with Endress+Hauser GmbH+Company KG, 79689 Maulburg, Germany.

Color versions of one or more of the figures in this letter are available online at http://ieeexplore.ieee.org.

Digital Object Identifier 10.1109/LMWC.2020.2970915

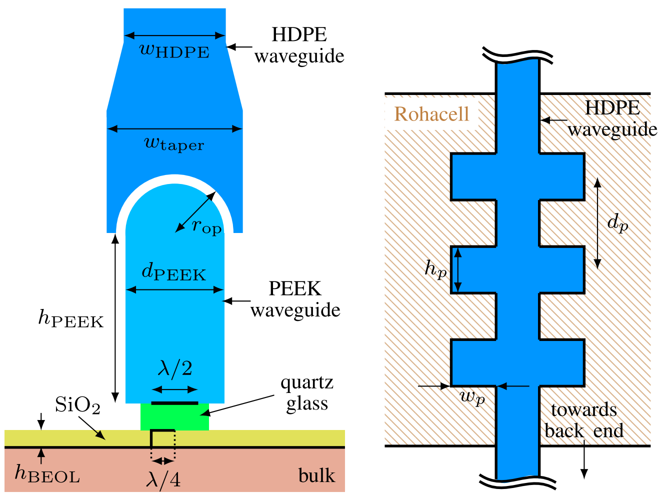

(a) (b)

Fig. 1. Schematic cross section of the transition from MMIC to (a) dielectric waveguide and (b) Rohacell holder.

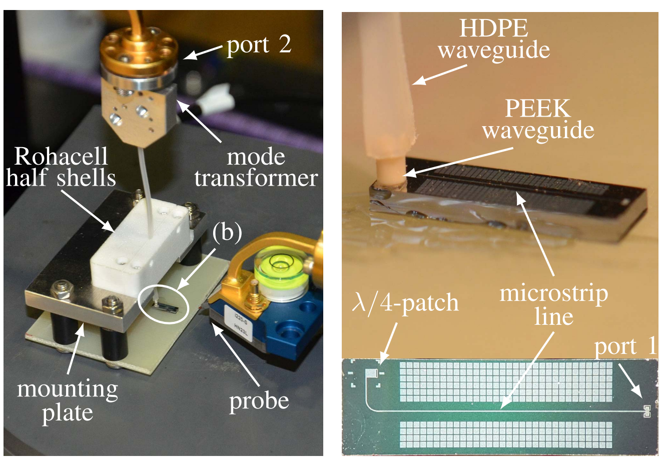

(a) (b)

Fig. 2. Realized transition from the back end to the flexible dielectric waveguide (a) in the measurement setup with Rohacell holder. (b) Detailed view on the transition and the BEOL layout.

enough to make the decoupling of the back end more efficient than the HDPE ($\varepsilon_r = 2.25$, $\tan\delta = 3.1 \cdot 10^{-4}$).

A self-aligning transition is used to connect the flexible and mechanically decoupled dielectric waveguide. The round waveguide dome is spherically rounded with a hemisphere. The counterpart in the flexible waveguide has a spherical opening with a radius r_{op} of 490 μm, aligning itself in the case of misalignment or mechanical stress. The hemispherical shapes serve not only for mechanical alignment but also for improved impedance matching. In order to avoid reflections at the interface, the wave impedance of the two dielectric waveguides is chosen to be very similar. The permittivity as well as the dimensions are the adjustable parameters. The flexible waveguide is made of HDPE and has a rectangular cross section of 648 μm × 1295 μm. A tapering to a cross section of 950 μm × 1295 μm decreases the IL of the transition and avoids additional radiation losses. Full-wave simulations of the transition from the back end to the flexible waveguide result

TABLE I

DIMENSIONS FOR THE TRANSITION IN MICROMETER

w_{patch}	l_{patch}	h_{PEEK}	w_{taper}	h_p	w_p	d_p
260	360	1000	950	750	1000	1750

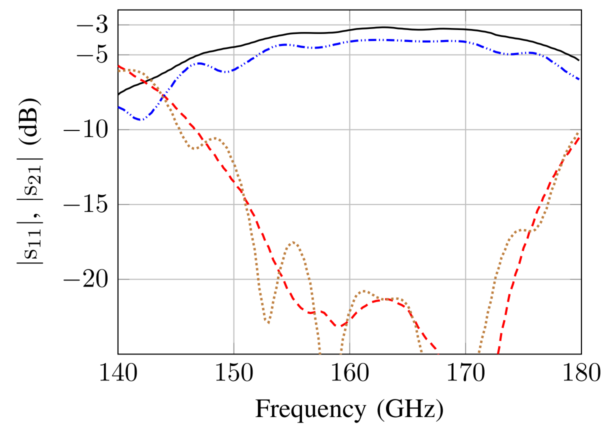

Fig. 3. Simulated S-parameters for the transition from the back end to the flexible waveguide without holder [$|s_{21}|$ (——), $|s_{11}|$ (- - - -)] and with holder [$|s_{21}|$ (-·-·-·), $|s_{11}|$ (········)].

in a minimum simulated IL of 3.1 dB with a 10-dB return loss bandwidth of 34 GHz, as shown in Fig. 3. The losses are mainly caused by the dielectric and metallic losses on the MMIC (70%) and only 23% by the radiation losses.

The requirements for the positioning precision of the quartz glass are high, and it should be positioned with 50 μm accuracy. The pluggable interface between the dome and the flexible front end, however, is very robust against the positioning tolerances due to the nonresonant coupling. A vertical displacement of 0.1 mm results in a larger air gap between the waveguide and the dome and reduces the transmission coefficient by 0.3 dB. Displacements in horizontal direction or slight tilting are even less critical.

Therefore, a Rohacell shell ($\varepsilon_r = 1.05$, $\tan\delta = 0.005$) is used to fix the flexible waveguide 1 cm above the BEOL MMIC. It disturbs the field distribution minimally and fits positively on a pin-shaped profile on the dielectric waveguide surface, as shown in Fig. 1(b). The pins fix the waveguide mechanically, but cause additional radiation losses. This increases the IL by approximately 0.9 dB (Fig. 3) on average. The transition dimensions are listed in Table I.

III. TRANSITION ASSEMBLY AND MEASUREMENTS

A BEOL MMIC was fabricated to characterize the transition. The quartz glass was metallized with a 2-μm-thick aluminum layer in a clean room process and glued on the BEOL MMIC with an epoxy adhesive. The PEEK waveguide was fixed on the top with an epoxy adhesive. The flexible waveguide was clamped with two Rohacell half shells and aligned over the PEEK waveguide using an aluminum mounting plate and screws. The realized transition is shown in Fig. 2.

For the S-parameter measurements, the BEOL MMIC was contacted with a probe, and the flexible dielectric waveguide was connected via a mode converter with a metallic

TABLE II
COMPARISON OF THE STATE-OF-THE-ART DESIGNS FOR TRANSITIONS FROM CHIP TO DIELECTRIC WAVEGUIDE

Ref.	Transition Design	Area (λ_0^2)	Substrate, Height	Frequency (GHz) [rel. Bandwidth]	Permittivity Waveguide	IL (dB)
[4]	self-aligned resonator	0.028	BCB ($\varepsilon_r = 2.55$), 24 µm	100 [7.2]	9.8	2.15
[5]	open-ended microstrip feed	0.07	BCB, 20 µm	175 [12]	11.9	3.2
[6]	half-mode SIW	0.189	SiO_2, 10 µm	275 [18.2]	6.15	4.8
[11]	bow-tie dipole with metal reflector	0.07	SiO_2, 10 µm	120 [15]	2.1	11
[14]	SIW on PCB fed by flip-chip	-	Megtron6 ($\varepsilon_r = 3.6$), 300um	120 [25]	2.1	3.4
This work	shortened $\lambda/4$-patch feeding a stacked design	0.01	SiO_2, 10 µm	160 [18.8]	2.25	3.0

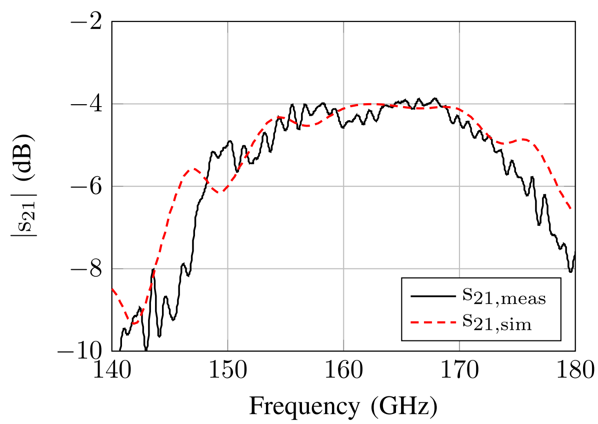

Fig. 4. Measured and simulated transmission coefficient $|s_{21}|$.

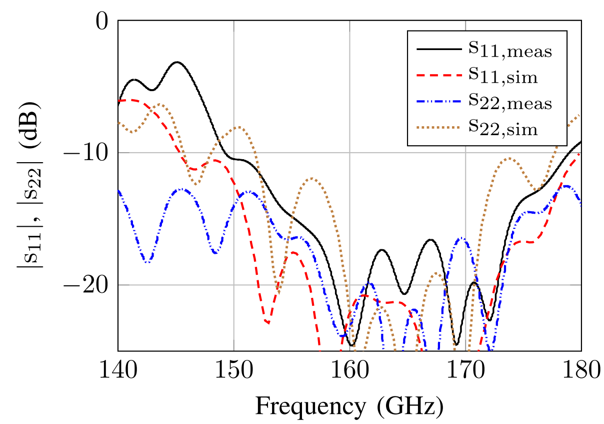

Fig. 5. Measured and simulated reflection coefficients $|s_{11}|$ (toward probe) and $|s_{22}|$ (toward rectangular waveguide).

waveguide. The S-parameters of the transition are determined by deembedding the measured losses of the microstrip line (6.9 dB $\hat{=}$ 1 dB/mm), the mode converter (0.5 dB) [2], and the flexible dielectric waveguide (0.3 dB), since the calibration reference plane was at the probe tip (s_{11}) or the waveguide interface (s_{21}, s_{22}).

The simulated and measured transmission coefficients are shown in Fig. 4. The maximum measured transmission coefficient is −3.9 dB at 168 GHz. In the frequency range from 147 to 177 GHz, the transmission coefficient declines by 3 dB compared to the measured maximum. The measured values agree very well with the simulations. According to the simulations, the Rohacell form has an IL of 0.9 dB. Deembedding this loss increases the transmission coefficient of the transition to −3.0 dB.

On the probe side, the measured reflection coefficient $|s_{11}|$ is below −10 dB in the frequency range from 149 to 179 GHz, as shown in Fig. 5. The reflection coefficient towards the waveguide is below −10 dB for the complete measured frequency range. Simulations and measurements agree well.

IV. Comparison With the State-of-the-Art Designs

The comparison of the proposed transition to the state-of-the-art designs must consider not only the IL and chip area but also the mechanical construction, material properties, and the realization of the BEOL MMIC. Several transitions are listed in Table II and subdivided into rigid dielectric waveguides with high permittivity [4]–[6] and flexible, low-permittivity waveguides [11], [14].

The presented transition has the lowest area consumption with a very small guard area (patch size plus 20 µm) around the patch and is fabricated with a commercial available IC process like [6], [11], [14]. With a relative bandwidth of 18.8%, the transition is very broadband. The measured IL of 3 dB is comparatively low. Transitions with comparable or lower insertion losses use higher low-loss substrates and high-permittivity dielectric waveguides, which improves the transition performance. Furthermore, the presented transition is mechanically decoupled, can be reconnected several times, and is even self-aligning, reducing the requirements concerning the positioning accuracy.

V. Conclusion

In this letter, a transition from MMIC to a flexible dielectric waveguide in the *G*-Band is presented. The transition is mechanically decoupled and aligns itself in the case of slight positioning tolerances.

The transition is based on a stacked design made out of several components. A resonant $\lambda/2$-patch, excited by the MMIC, feeds the fundamental HE_{11} mode into a rigid dielectric waveguide. By rounding the rigid waveguide end spherically, the flexible waveguide can be aligned with the corresponding counterpart above it. Rohacell half shells are used to fix the flexible waveguide. The minimum measured IL without the Rohacell holders is 3 dB at 168 GHz. The transition is matched better than 10 dB over a bandwidth of 30 GHz.

REFERENCES

[1] S. Fukuda *et al.*, "A 12.5+12.5 Gb/s full-duplex plastic waveguide interconnect," *IEEE J. Solid-State Circuits*, vol. 46, no. 12, pp. 3113–3125, Dec. 2011.

[2] M. Geiger, M. Hitzler, J. Iberle, and C. Waldschmidt, "A dielectric lens antenna fed by a flexible dielectric waveguide at 160 GHz," in *Proc. 11th Eur. Conf. Antennas Propag. (EUCAP)*, Mar. 2017, pp. 3380–3383.

[3] M. Geiger and C. Waldschmidt, "160-GHz radar proximity sensor with distributed and flexible antennas for collaborative robots," *IEEE Access*, vol. 7, pp. 14977–14984, 2019.

[4] U. Dey and J. Hesselbarth, "Building blocks for a millimeter-wave multiport multicast chip-to-chip interconnect based on dielectric waveguides," *IEEE Trans. Microw. Theory Techn.*, vol. 66, no. 12, pp. 5508–5520, Dec. 2018.

[5] B. Yu *et al.*, "Ortho-mode sub-THz interconnect channel for planar chip-to-chip communications," *IEEE Trans. Microw. Theory Techn.*, vol. 66, no. 4, pp. 1864–1873, Apr. 2018.

[6] J. W. Holloway, L. Boglione, T. M. Hancock, and R. Han, "A fully integrated broadband sub-mmWave chip-to-chip interconnect," *IEEE Trans. Microw. Theory Techn.*, vol. 65, no. 7, pp. 2373–2386, Jul. 2017.

[7] B. Yu, Y. Liu, Y. Ye, X. Liu, and Q. J. Gu, "Low-loss and broadband G-band dielectric interconnect for chip-to-chip communication," *IEEE Microw. Wireless Compon. Lett.*, vol. 26, no. 7, pp. 478–480, Jul. 2016.

[8] B. Yu, Y. Liu, Y. Ye, J. Ren, X. Liu, and Q. J. Gu, "High-efficiency micromachined sub-THz channels for low-cost interconnect for planar integrated circuits," *IEEE Trans. Microw. Theory Techn.*, vol. 64, no. 1, pp. 96–105, Jan. 2016.

[9] U. Dey and J. Hesselbarth, "Millimeter-wave multicast chip-to-chip interconnect network using dielectric slab waveguide," in *IEEE MTT-S Int. Microw. Symp. Dig.*, Jun. 2018, pp. 378–381.

[10] Y. Kim, L. Nan, J. Cong, and M.-C.-F. Chang, "High-speed mm-wave data-link based on hollow plastic cable and CMOS transceiver," *IEEE Microw. Wireless Compon. Lett.*, vol. 23, no. 12, pp. 674–676, Dec. 2013.

[11] N. Van Thienen, Y. Zhang, and P. Reynaert, "Bidirectional communication circuits for a 120-GHz PMF data link in 40-nm CMOS," *IEEE J. Solid-State Circuits*, vol. 53, no. 7, pp. 2023–2031, Jul. 2018.

[12] N. Van Thienen, W. Volkaerts, and P. Reynaert, "A multi-gigabit CPFSK polymer microwave fiber communication link in 40 nm CMOS," *IEEE J. Solid-State Circuits*, vol. 51, no. 8, pp. 1952–1958, Aug. 2016.

[13] M. Hitzler, S. Saulig, L. Boehm, W. Mayer, and C. Waldschmidt, "MMIC-to-waveguide transition at 160 GHz with galvanic isolation," in *IEEE MTT-S Int. Microw. Symp. Dig.*, May 2016, pp. 1–4.

[14] N. Van Thienen, Y. Zhang, M. De Wit, and P. Reynaert, "An 18 Gbps polymer microwave fiber (PMF) communication link in 40 nm CMOS," in *Proc. Conf. 42nd Eur. Solid-State Circuits Conf. (ESSCIRC)*, Sep. 2016, pp. 483–486.

[15] J. Hasch, U. Wostradowski, S. Gaier, and T. Hansen, "77 GHz radar transceiver with dual integrated antenna elements," in *German Microw. Conf. Dig. Papers*, Mar. 2010, pp. 280–283.